Thermal Model of the Output Traction Converter of an Electric Locomotive with Induction Motors

Goolak S.[1], Kyrychenko M.[2]
[1]State University of Infrastructure and Technologies
Kyiv, Ukraine
[2]Kyiv National University of Construction and Architecture
Kyiv, Ukraine

Abstract. The aim of research is to develop a thermal model of the output converter of an electric locomotive with vector control, taking into account the operating modes of the electric locomotive. The aim was achieved by using energy losses at the moments of switching functions that describe the nature of the change in the curves of currents and power voltages of transistors and converter diodes. The object of research is an autonomous voltage converter, which is part of the traction drive of an electric locomotive with a vector control system. The simulation was carried out for an autonomous voltage converter, the load of which is two traction induction motors operating in the nominal mode. The temperature of transistors and diodes is obtained for the established modes of operation of traction motors. The most important results are the analytical dependence of thermal power losses in the inverter as a function of inverter phase currents and voltages. The significance of the results obtained is to establish the dependence of the temperature of the power devices of the inverter on the actual operating conditions of the electric locomotive. The established dependencies will further determine the spectral power of thermal noise. This will allow, when designing a traction drive control system, to develop an effective system for filtering thermal noise. This will increase the energy performance of the traction drive of the electric locomotive by improving the accuracy of regulation.
***Keywords*:** heat loss energy, diagnostics, induction motor, mathematical modeling, autonomous voltage inverter, temperature, thermal resistance.

DOI: https://doi.org/10.52254/1857-0070.2022.3-55.01
UDC: 621.313.333.2

Model termic al convertorului de tracțiune de ieșire al locomotivei electrice cu motoare asincrone

Gulac S.A.,, Kiricenko M.A.
[1]Universitatea de Stat de Infrastructură și Tehnologie
Kiev, Ucraina
[2]Universitatea Națională de Construcții și Arhitectură din Kiev
Kiev, Ucraina

Rezumat. Scopul lucrării este elaborarea modelului termic a unui invertor de tensiune autonom cu control vectorial al unei locomotive electrice, ținând cont de modurile de funcționare ale locomotivei electrice. Scopul a fost atins prin utilizarea funcțiilor care descriu natura modificării curbelor de curent și tensiune ale tranzistoarelor și diodelor de putere ale unui invertor de tensiune autonom, atunci cînd se calulează pierderile de energie în momentul comutării. Ca obiect de studiu a fost ales un invertor de tensiune autonom cu sistem de control vectorial, care face parte din unitatea de tracțiune a unei locomotive electrice pentru motoarele de tracțiune asincrone, cu caracteristici de bază bine cunoscute. Simularea a fost efectuată pentru un invertor autonom de tensiune, a cărui sarcină este două motoare asincrone de tracțiune care funcționează în modul nominal. Temperatura tranzistoarelor și diodelor a fost obținută pentru funcționarea în regim de echilibru a motoarelor asincrone de tracțiune. Cel mai important rezultat este dependența analitică a pierderilor de putere termică în invertor, în funcție de curenții de fază și tensiunile invertorului. Semnificația rezultatelor constă în stabilirea dependențelor temperaturii dispozitivelor electronice ale invertorului în condițiile de funcționare reale a locomotivei electrice. Dependențele stabilite vor determina în continuare puterea spectrală a zgomotului termic. Acest lucru va îmbunătăți exactitatea reglării parametrilor controlați ai sitemului de tracțiune care, la rîndul său va îmbunătăți performanța energetică ai unității de tracțiune a locomotivei electrice prin reducerea pierderilor în sistemul de tracțiune.
***Cuvinte-cheie*:** energie, pierderi de căldură, diagnosticare, motor asincron, modelare matematică, invertor de tensiune autonom, temperatură, rezistență termică.

Тепловая модель выходного тягового преобразователя электровоза с асинхронными двигателями

Гулак С.А.[1], Кириченко М.А.[2]
[1]Государственный университет инфраструктуры и технологий
Киев, Украина
[2]Киевский национальный университет строительства и архитектуры,
Киев, Украина

Аннотация. Целью работы является разработка тепловой модели автономного инвертора напряжения электровоза с векторным управлением с учетом эксплуатационных режимов работы электровоза. Поставленная цель была достигнута за счет применения при расчете потерь энергии в моменты коммутации функций, описывающих характер изменения кривых токов и напряжения силовых транзисторов и диодов автономного инвертора напряжения. В качестве объекта исследования был выбран автономный инвертор напряжения, входящий в состав тягового привода электровоза с векторной системой управления асинхронными тяговыми двигателями, с известными паспортными характеристиками. Моделирование проводилось для автономного инвертора напряжения, нагрузкой которому служат два тяговых асинхронных двигателя, работающие в номинальном режиме. Температура транзисторов и диодов была получена для установившихся режимов работы тяговых асинхронных двигателей с учетом работы системы охлаждения и взаимного теплового влияния указанных электронных приборов. Наиболее важными результатами являются полученная аналитическая зависимость тепловых потерь мощности в автономном инверторе напряжений, как функции фазных токов и напряжений инвертора, получение аналитической зависимости для определения параметров тепловой модели электронного прибора, как функций коэффициентов аппроксимации кривой теплового сопротивления прибора, учет влияния системы охлаждения, используемой на электровозе, на температуру электронных приборов. Значимость полученных результатов состоит в установлении зависимостей температуры силовых электронных приборов автономного инвертора напряжения от реальных условий эксплуатации электровоза. Установленные зависимости позволят в дальнейшем определить спектральную мощность тепловых шумов в векторной системе управления тяговым приводом электровоза для построения эффективной системы фильтрации тепловых шумов. Это позволит повысить точность регулирования контролируемых параметров тягового привода, что, в свою очередь, позволит повысить энергетические показатели тягового привода электровоза за счет уменьшения потерь в тяговом приводе.

Ключевые слова: энергия тепловых потерь, диагностика, асинхронный двигатель, математическое моделирование, автономный инвертор напряжения, температура, тепловое сопротивление.

INTRODUCTION

On electric locomotives with an induction traction drive, a vector control system for traction motors has become widespread [1, 2]. The energy efficiency of the drive depends on the accuracy of controlling the operation of the traction drive [3]. This circumstance is connected with the fact that the optimization of the control system operation according to the energy criterion leads to a decrease in losses in the drive and, as a result, to an increase in the power factor and efficiency factor of the drive as a whole [4].

An analysis of the structure of a traction drive with vector control of induction traction motors shows that the main power losses occur in induction motors, a rectifier, a smoothing reactor, and an autonomous voltage inverter [5]. In this work, the authors conditionally divide the energy losses in the traction drive into constant and variable. Constant power losses are losses in the steady state operation of the drive, variable losses are losses that occur during transient processes [6].

In [7], it is indicated that the energy of losses in the elements of the traction drive is converted into thermal energy, which leads to heating of these elements, in particular, an autonomous voltage inverter. This circumstance leads to the fact that with an increase in the temperature of electronic switches of an autonomous voltage inverter, such as power thyristors, power transistors, the thermal noise of these devices increases [8]. The presence of thermal noise in the electronic keys of an autonomous inverter reduces the accuracy of regulation of parameters controlled by the vector control system, which leads to an increase in losses in the traction drive system of an electric locomotive [9].

To build an efficient thermal noise filtering system, it is necessary to determine noise parameters, such as mathematical expectation and dispersion, which are functions of the temperature of an autonomous voltage inverter. To this end, it is necessary to develop a thermal model of an autonomous voltage inverter, taking into account losses both in steady state and in transient operating modes.

When constructing a thermal model of an autonomous voltage inverter, it is necessary to develop a thermal model for the operation of its electronic modules. In traction drives of electric locomotives, IGBT transistors and power diodes are mainly used as electronic modules in autonomous voltage inverters [10].

При построении тепловых моделей IGBT

When building thermal models of IGBT transistors and power diodes, certain difficulties arise. These difficulties are associated with the fact that transient processes in these electronic devices last several hundred nanoseconds [11]. The interval between commutations of the transistor and the diode is of the order of several milliseconds. To obtain an adequate result in modeling, it is necessary to choose a step equal to several picoseconds, which will lead to a large amount of calculations [12].

The solution to this problem can be found in [13]. In this paper, the authors proposed a 3D thermal transient modeling method suitable for designing power electronics systems that takes into account both non-uniform power losses and cooling conditions. Despite the obviously correct approach to the problem posed, the losses in the transistor and diode at the moment of switching and the mutual influence of the transistor and diode temperatures were not considered in [13]. This will lead to incorrect determination of losses at the specified moments of operation of an autonomous voltage inverter.

In [14], a thermal model was proposed that takes into account the mutual influence of the temperature of the transistor and diode when determining thermal losses, but the question of determining thermal losses in IGBT modules at the moments of switching remains open.

The authors of [15], when developing a thermal model, proposed a method that allows taking into account thermal losses at the moment of switching. In addition, during the development of the model, they established a relationship between the thermal characteristics of the parameters and the operating parameters of the IGBT modules. But, this work does not take into account the mutual influence of the temperature of the transistor and diode on the losses in the IGBT module. In addition, in [15], the thermal model of the IGBT module was built taking into account only the first harmonic of the load current. In autonomous inverters with pulse-width modulation (PWM), the spectrum of the load current also contains higher harmonic components of the load current. This factor reduces the scope of the proposed model.

In the [16], a thermal model of a three-phase voltage inverter is presented, which takes into account losses in IGBT modules. Also in this work, the influence of a heat sink for heat removal on the temperature of IGBT modules is taken into account. However, the work does not take into account the influence of the cooling medium.

The paper proposes a thermal model of an autonomous voltage inverter, which makes it possible to determine the temperature of the IGBT modules of the inverter. The thermal model takes into account power losses in IGBT modules, taking into account switching, the mutual influence of the temperature of the transistor and diode on power losses in the module, and uneven cooling of IGBT modules by the cooling medium.

The results of this work can be used in the design of a traction drive for electric locomotives with a vector control system to take into account the influence of thermal noise of an autonomous voltage inverter.

The aim of the study is to create a thermal model of an autonomous voltage inverter, which is part of the traction drive of an electric locomotive with vector control, taking into account the actual operating conditions of the electric locomotive.

This work differs from the known ones in that when developing the thermal model of the inverter, time functions were proposed that describe the behavior of the curves of currents and voltages of electronic devices at characteristic time intervals. This made it possible to obtain an analytical expression for losses as a function of phase currents and voltages of the inverter. In addition, the use in the model as a load of induction traction motors and cooling conditions, which is used on an electric locomotive, made it possible to take into account the real operating conditions of an electric locomotive.

DEVELOPMENT OF THE STRUCTURAL DIAGRAM OF THE THERMAL MODEL OF THE IGBT MODULE

As an object of research, a traction drive with vector control of induction motors of the DC-3 electric locomotive (Ukraine) was adopted. Passport parameters of an autonomous inverter, which is part of the traction drive of the DC-3

electric locomotive, are given in Table 1. BSM200GA120DN2 modules are used as an IGBT module in an autonomous voltage inverter, the passport characteristics of which are given in Table 2.

Table 1.

Passport parameters of autonomous voltage inverter of DC-3 electric locomotive

Parameter	Designation	Unit	Value
Instantaneous value of rated phase voltage	U_n	V	1527
Instantaneous value of rated phase current	I_n	A	450
IGBT module type: BSM200GA120DN2			
Number of IGBT modules	N_{module}	pcs.	6
Number of IGBT modules on one radiator	n_{module}	pcs.	2
Radiator area	S_r	mm^2	570×450
Radiator material: Aluminum			
Cooling type: liquid			
Coolant: mixture of water and antifreeze	x_1	Ohm	0.56
Maximum coolant temperature	T_{max}	°C	+55
Minimum coolant temperature	T_{min}	°C	-40

Table 2.

Passport parameters of IGBT module BSM200GA120DN2

Parameter	Designation	Unit	Value
Transistor			
Collector-emitter voltage	U_{CE}	V	1200
Collector-gate voltage R_{GE}=20 kΩ	U_{CGE}	V	1200
Gate-emitter voltage	U_{GE}	V	±20
DC collector current			
T_C=25 °C	I_C	A	300
T_C=80 °C	I_C	A	200
Pulsed collector current, t_p=1ms			
T_C=25 °C	I_{Cpulse}	A	600
T_C=80 °C	I_{Cpulse}	A	400
Power dissipation per IGBT T_C=25 °C	P_{tot}	W	1550
Chip temperature	T_j	°C	150
Storage temperature	T_{stg}	°C	-40…125
Collector-emitter saturation voltage			
U_{GE}=15 V, I_C=200 A, T_j=25 °C	$U_{CE(sat)}$	V	2.5
U_{GE}=15 V, I_C=200 A, T_j=125 °C	$U_{CE(sat)}$	V	3.1
Zero gate voltage collector current			
U_{CE}=1200 V, U_{GE}=0 V, T_j=25 °C	I_{CES}	mA	3
U_{CE}=1200 *V*, U_{GE}=0 V, T_j=125 °C	I_{CES}	mA	12
Switching Characteristics, Inductive Load at T_j=125 °C, U_{CE}=600 V, U_{GE}= -15 V, I_C=200 A			
Turn-on delay time, R_{Gon}=4.7 Ω	$t_{d(on)}$	ns	110
Rise time, R_{Gon}=4.7 Ω	t_r	ns	80
Turn-off delay time, R_{Goff}=4.7 Ω	$t_{d(off)}$	ns	550
Fall time, R_{Goff}=4.7 Ω	t_f	ns	80
Free-Wheel Diode,			
Diode forward voltage			
I_f=200 A, U_{GE}=0 V, T_j=25 °C	U_F	V	2.3
I_f=200 A, U_{GE}=0 V, T_j=125 °C	U_F	V	1.8

Reverse recovery time, I_f=200 A, U_R=-600 V, U_{GE}=0 V, di_1/dt=-2000 A/μs, T_j=25 °C	t_{rr}	μs	0.5

The scientific approach to compiling a thermal model of an autonomous voltage inverter is schematically shown in fig. 1 in block diagram form.

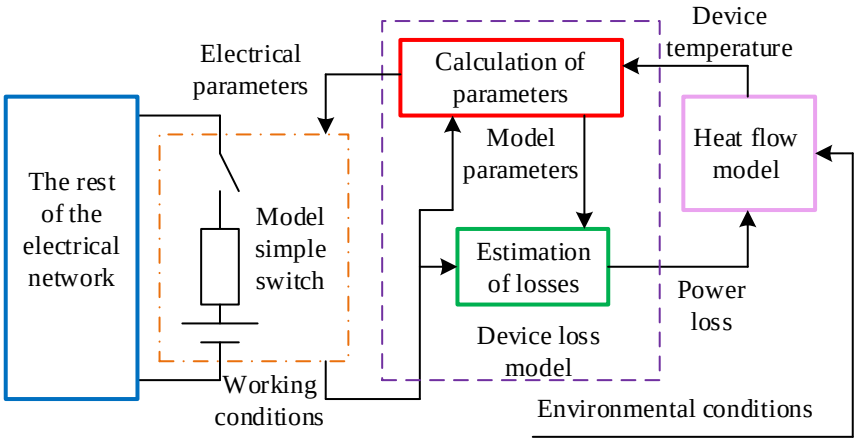

Fig. 1. Structural diagram of the thermal model of an autonomous voltage inverter

Losses in the device are estimated by observing currents and voltages before and after switching according to the algorithm described below. These losses become input to the dynamic model of the heat control system (heat flow), which calculates temperature changes in different parts of the system. Because device loss is a function of temperature, the computed device temperature is used to modify the switch loss model parameters for the next time step.

LOSS MODEL IN IGBT MODULE

The losses of an IGBT module can be divided into conduction losses, turn-on switching losses, turn-off switching losses, and off-state losses [17]. Losses in the conduction mode are determined by the formula [17]

$$P_{cond} = I_C \cdot U_{CE(sat)}, \quad (1)$$

where I_C - collector current;

$U_{CE(sat)}$ - forward saturation voltage (Table 2).

Losses in the off state are determined by the formula [17]

$$P_{blok} = I_{CES} \cdot U_{CE}, \quad (2)$$

where I_{CES} - leakage current (Table 2);

U_{CE} - blocking voltage (Table 2).

Determining the switching loss is a difficult task because the duration of the switching process is several hundred nanoseconds. The authors propose a workaround for this situation by applying algebraic equations representing the voltage and current waveforms during the switching process based on the fact that the current and voltage waveforms during switching are basically a function of the voltage before, after the switch and the current value. The parameters of these equations are derived from the equations of voltage, current and other physical quantities before and after switching. Energy losses are calculated analytically by integrating the product of the developed voltage and current equations, which leads to the switching loss formula. Thus, the simulation can be performed with a large time step, while the developed formula provides an estimate of the losses for each switching.

The switching loss model developed in this article is applicable to "hard-switched" IGBT modules widely used in modern power electronics. Each switch consists of an IGBT with a freewheeling diode connected in parallel. The turn-on of the IGBT (and hence the turn-on loss of switching) is significantly affected by the nature of the recovery of the freewheeling free diode and parasitic inductance.

As noted above, the turn-on loss of an IGBT is affected by the recovery characteristics of the freewheeling diode. The waveforms when the diode is turned off are shown in fig. 2. As the diode current drops, some of its accumulated charge is removed due to recombination. The amount of charge removed is a function of the

rate of change of current dI_d / dt. This speed is determined by the turn-on speed of the IGBT at the reverse terminal of the diode. The rest of the accumulated charge is actively removed by the negative current flowing through the diode. During the initial period of this process, known as reverse recovery, the negative current rises; with the development of a reverse voltage that occurs only when the current reaches the peak value of the reverse recovery current (I_{rrm}). In the developed model, the parameters I_{rrm} and t_{rr} (the time required for reverse recovery) are used as input data.

The voltage and current curves when the diode is turned off are selected taking into account three different intervals shown in fig. 3. On the interval $\left[t_{0(rec)} - t_{2(rec)}\right]$, I_d, is modeled as a linear slope, which is described by the formula

$$I_d(t) = -I'_{1(rec)} \cdot \left(t - t_{1(rec)}\right) \cdot e^{-\alpha_1(rec)\cdot\left(t-t_{1(rec)}\right)^2}, \quad (3)$$

where

$$k_D = \frac{I_{rrm}\cdot\sqrt{e}}{t_{rr}\cdot\left(\frac{dI_d}{dt}\Big|t_0\right)}, \quad (4)$$

$$\alpha_{1(rec)} = \frac{1}{\left(t_{rr}\cdot k_D\right)^2}, \quad (5)$$

$$I'_{1(rec)} = \sqrt{2\cdot\alpha_{1(rec)}}\cdot I_{rrm}\cdot\sqrt{e}. \quad (6)$$

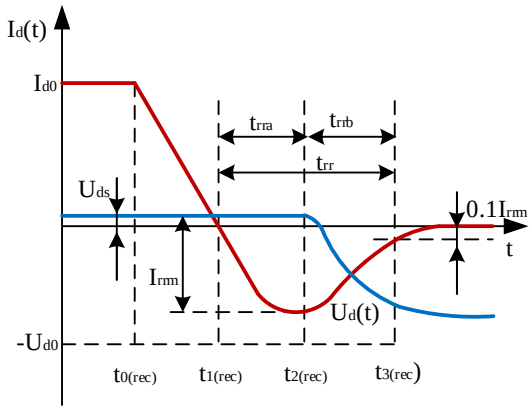

Fig. 2. Idealized current $(I_d(t))$ and voltage $(U_d(t))$ curves of the diode turn-off transient.

On the interval $\left[t_{0(rec)} - t_{2(rec)}\right]$, the voltage U_d is modeled by a straight line, the equation of which is

$$U_d(t) = U_{ds} = U_{CE}. \quad (7)$$

On the interval $t > t_{2(rec)}$, the current and voltage are modeled as follows

$$I_d(t) = I_{rrm}\cdot e^{-2\cdot\alpha_2(rec)\cdot\left(t-t_{1(rec)}\right)^2}, \quad (8)$$

$$U_d(t) = U_{1(rec)}\cdot e^{-\alpha_2(rec)\cdot\left(t-t_{1(rec)}\right)^2} - U_{d0}, \quad (9)$$

where

$$U_{1(rec)} = U_{ds} + U_{d0}. \quad (10)$$

The condition that the reverse recovery current decreases to 10% I_{rrm} after time t_{rr} is given by

$$\alpha_{2(rec)} = \frac{\ln(10)}{t_{rrb}^2} = \frac{\ln(10)}{\left(1-k_D\right)^2\cdot t_{rr}^2}. \quad (11)$$

The times $t_{1(rec)}$, $t_{2(rec)}$, and $t_{3(rec)}$ are determined by the formulas

$$t_{1(rec)} = t_{0(on)} + t_{d(on)} - \frac{1}{8}\cdot t_r. \quad (12)$$

$$t_{2(rec)} = t_{1(rec)} + \frac{10}{8}\cdot t_r. \quad (13)$$

$$t_{3(rec)} = t_{2(rec)} + k_D\cdot t_{rr}. \quad (14)$$

Based on the above relations, the curves of the current and voltage of the diode at the moment of its disconnection were plotted (Fig. 3).

Then the energy loss can be calculated as follows

$$W_{rec} = \int_{t_{0(rec)}}^{t_{2(rec)}} U_d(t)\cdot I_d(t)dt + \int_{t_{2(rec)}}^{t_{3(rec)}} U_d(t)\cdot I_d(t)dt. \quad (15)$$

By changing the values of the current flowing through the diode from 50 A to 400 A, at U_{d0}, equal to 600 V, the energy loss curve was plotted when the diode is turned off (Fig. 4). In fig. 4 also plotted the curve of energy losses when the

diode is turned off, corresponding to the passport characteristics.

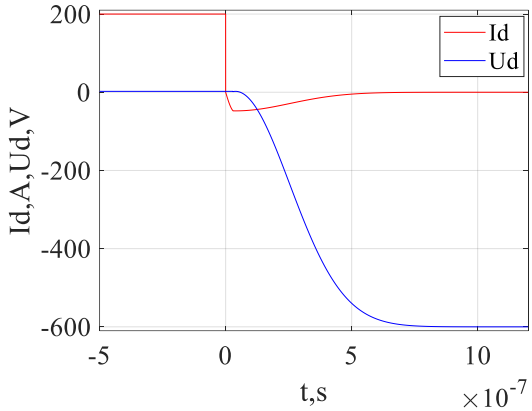

Fig. 3. Curves of current $(I_d(t))$ and voltage $(U_d(t))$ of the transient turning off the diode.

The error in determining the losses when the diode is turned off is calculated by the formula

$$\sigma_{rec} = \frac{\sqrt{\sum_{i=1}^{N}\left(W_{rec.calc} - W_{rec.ideal}\right)^2}}{N} \cdot 100\%, \qquad (16)$$

where $W_{rec.calc}$ – the energy losses when the diode is turned off, calculated by formula (15);
$W_{rec.ideal}$ – passport energy losses when the diode is turned off;
N – the number of readings.

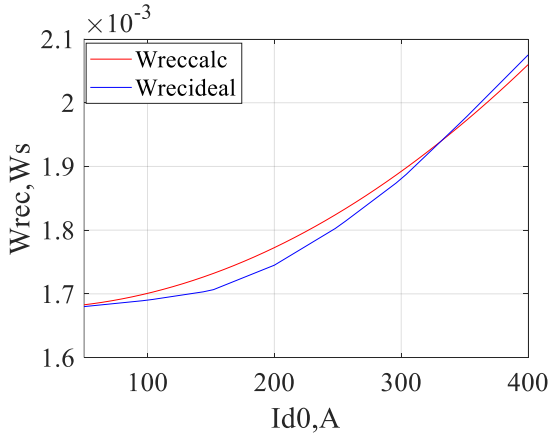

Fig. 4. Energy losses when the diode is turned off: calculated $(W_{reccalc})$ and passport $(W_{recideal})$.

Fig. 5 shows waveforms for an IGBT hard-on transient. In the data sheets, the switch-on process is characterized by switch-on delay time $t_{d(on)}$, rise time and switch-on energy.

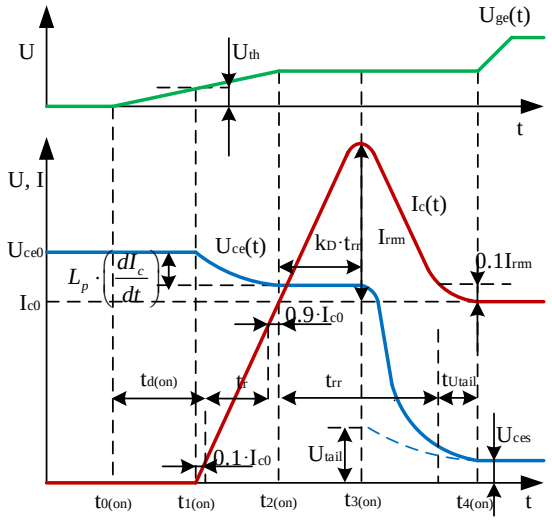

Fig. 5. Idealized current $(I_C(t))$ and voltage $(U_{ce}(t))$ of the transient turning on the transistor.

The error in determining the energy loss when the diode was turned off was $\sigma = 12\%$, which indicates a high degree of reliability of the calculated parameters.

The gate turn-on pulse is applied at $t_{0(on)}$, which causes the gate voltage U_{ge} to rise gradually (through the input capacitance of the IGBT). After a while $t_{d(on)}$, when U_{ge} reaches the threshold voltage U_{th}, the collector current I_C begins to rise almost linearly, and the load current from the freewheel diode gradually passes to the IGBT. During this rise, the voltage of the device (collector-emitter) $U_{ce}(t)$ undergoes a drop, primarily due to parasitic inductance (L_p).

The overshoot I_C during $\left[t_{2(on)} - t_{4(on)}\right]$ is due to the reverse recovery current of the freewheeling diode. The collector-emitter voltage U_{ce} begins to drop when the freewheel recovery current reaches its peak value at time $t_{3(on)}$.

The transition process of turning on the transistor is divided into three intervals $\left[t_{1(on)} - t_{2(on)}\right]$, $\left[t_{2(on)} - t_{3(on)}\right]$ and $\left[t_{3(on)} - t_{4(on)}\right]$

(Fig. 5). The boundaries of time intervals are determined by the formulas

$$t_{1(on)} = t_{0(on)} + t_{d(on)} - 0.25 \cdot t_r. \quad (17)$$

$$t_{2(on)} = t_{1(on)} + \frac{10}{8} \cdot t_r. \quad (18)$$

$$t_{3(on)} = t_{2(on)} + k_D \cdot t_{rr}. \quad (19)$$

$$t_{4(on)} = t_{2(on)} + t_{rr} + t_{U_{tail}}. \quad (20)$$

On the interval $\left[t_{1(on)} - t_{2(on)}\right]$ I_C and U_{ce} defined as

$$I_c(t) = I_{c1(on)} \cdot \left(1 - e^{-\alpha_{1(on)} \cdot \left(t - t_{1(on)}\right)}\right), \quad (21)$$

$$U_{ce}(t) = U_{ce0} - U_{1(on)} \cdot \left(1 - e^{-\lambda_{1(on)} \cdot \left(t - t_{1(on)}\right)}\right). \quad (22)$$

Taking into account the almost linear growth of the current, it is assumed that $I_{1(on)} \approx 100 \cdot I_{C0}$, where I_{C0} – the on-state current. Then

$$\alpha_{1(on)} = \frac{1}{1.25 \cdot t_r} \cdot \ln\left|\frac{1}{0.99}\right|. \quad (23)$$

Approximate value for $U_{1(on)}$ obtained by taking into account the average value dI_C / dt through parasitic inductance L_p

$$U_{1(on)} = \frac{8 \cdot I_{c0}}{9 \cdot t_r} \cdot L_p. \quad (24)$$

The coefficient $\lambda_{1(on)}$ is obtained under the condition of a 90% decline $U_{1(on)}$ during the period under review

$$\lambda_{1(on)} = \frac{1}{1.25 \cdot t_r} \cdot \ln 10. \quad (25)$$

On the interval $\left[t_{2(on)} - t_{3(on)}\right]$, the collector current is the sum of the load current and the recovery current of the freewheeling diode (3), while U_{ce} remains at the voltage level U_{cep} defined below

$$I_c(t) = I_{c0} + I'_{rec} \cdot \left(t - t_{2(on)}\right) \cdot e^{-\alpha_{1(rec)} \cdot \left(t - t_{2(on)}\right)^2}, \quad (26)$$

$$U_{cep}(t) = U_{ce0} - \frac{0.8 \cdot I_{c0}}{t_r} \cdot L_p. \quad (27)$$

After $t_{3(on)}$ the recovery current of the freewheeling diode gradually falls off in accordance with (3), while U_{ce} falling off to its saturation value U_{ces}. It is assumed that U_{ce} consists of two components droping at different rates

$$U_{ce}(t) = U_{2(on)} \cdot e^{-\alpha_{2(rec)} \cdot \left(t - t_{3(on)}\right)^2} + \\ + U_{3(on)} \cdot e^{-\lambda_{3(rec)} \cdot \left(t - t_{3(on)}\right)^2}, \quad (28)$$

$$I_c(t) = I_{c0} + I_{rrm} \cdot e^{-\alpha_{2(rec)} \cdot \left(t - t_{3(on)}\right)^2}. \quad (29)$$

The coefficient $U_{3(on)}$ is the slow drop U_{ce} component and is equal to the voltage U_{tail} shown in fig. 5 and looks roughly proportional to the level voltage U_{cep}. Thus, the coefficient $k_{U\infty} = \left[0 - 1\right]$ characterizing the value of the end of the characteristic is defined as follows

$$U_{tail} = k_{U\infty} \cdot U_{cep}. \quad (30)$$

Then the value of the rapidly fading component (dropping at the same rate as the recovery current of the freewheeling diode) is equal to

$$U_{2(on)} = \left(1 - k_{U\infty}\right) \cdot U_{cep}. \quad (31)$$

From the condition of the voltage drop at the end of the characteristic to the level U_{ces}, when $t_{4(on)}$ obtained

$$\lambda_{3(on)} = \frac{1}{\left(\left(1 - k_D\right) \cdot t_{rr} + t_{U_{tail}}\right)^2} \cdot \ln\left|\frac{k_{U\infty} \cdot U_{cep}}{U_{ces}}\right|. \quad (32)$$

Based on the above relations, the current and voltage curves of the transistor were plotted at the moment of its switching on (Fig. 6).

Then the energy loss when the transistor is turned on can be calculated as follows

$$W_{on} = \int_{t_{1(on)}}^{t_{4(on)}} U_{ce}(t) \cdot I_c(t)\, dt. \quad (33)$$

By changing the values of the current flowing through the transistor from 50 A to 400 A, at $U_{ce0} = 600\text{V}$, the energy loss curve was plotted when the transistor was turned on (Fig. 7). In fig. 7 also plotted the energy loss curve when the transistor is turned on, corresponding to the passport characteristics.

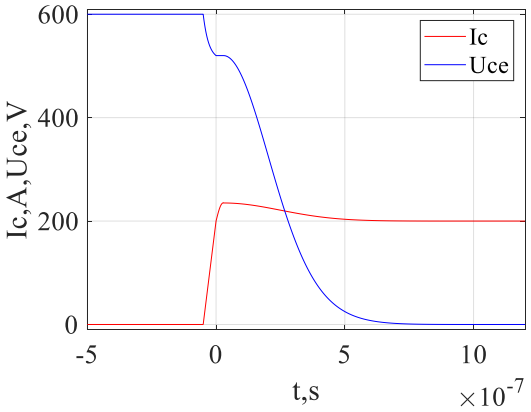

Fig. 6. Curves of current $(I_C(t))$ and voltage $(U_{ce}(t))$ of the transition process of turning on the transistor.

After replacing in formula (16) $W_{reccalc}$ with W_{oncalc} and $W_{recideal}$ with $W_{onideal}$ the error in determining the energy loss when the transistor is turned on, the value of which was $\sigma = 3.77\%$. This indicates a high degree of reliability of the calculated parameters.

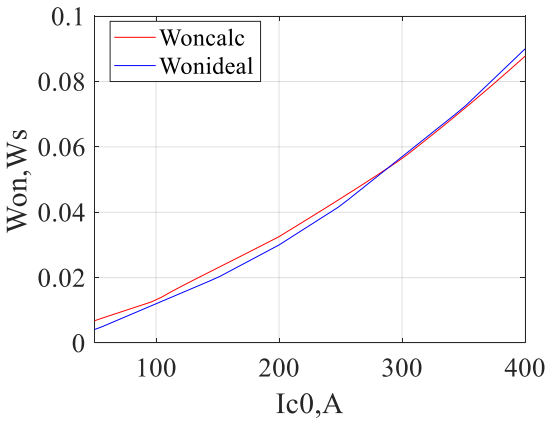

Fig. 7. Energy losses when the transistor is turned on: calculated (W_{oncalc}) and passport $(W_{onideal})$.

The IGBT shutdown process shown in fig. 8 is characterized in the technical data sheets by the trip delay time, $t_{d(off)}$, the delay time t_f and the trip energy W_{off}. The shutdown process begins after a negative voltage is applied to the gate at the moment t_0 (shutdown).

The input capacitance of the IGBT is discharged, gradually decreasing the gate-emitter voltage U_{ge}, but the collector-emitter voltage U_{ce} remains constant until U_{ge} drops enough to bring the IGBT out of saturation. This initial period is shown in Fig. 5 $t_{U_{d(off)}}$. After that, the collector-emitter voltage rises rapidly. When U_{ce} reaches the forward blocking voltage U_{ce0}, at $t_{2(off)}$, the reverse diode becomes forward biased and begins to take on the load current.

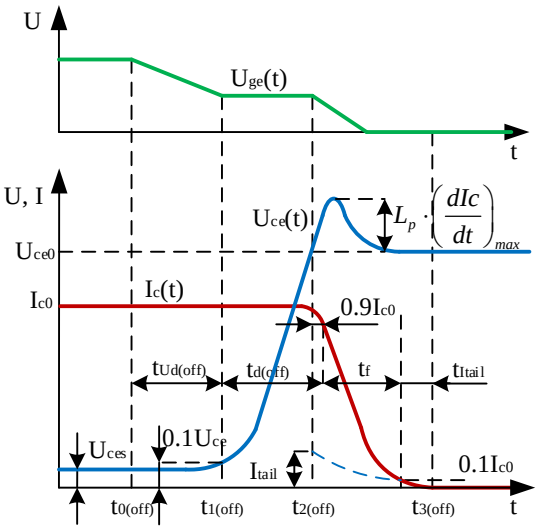

Fig. 8. Idealized current $(I_C(t))$ and voltage $(U_{ce}(t))$ transient turn off transistor.

The internal design of the IGBT includes a MOSFET driving a bipolar transistor, and through the mechanisms involved in these devices, the collector current I_C drops rapidly at first. Then this fall becomes smoother until fading at the moment $t_{3(off)}$. The rapid drop in current due to parasitic inductance causes overvoltage U_{ce}.

The expressions for current and voltage when the transistor is turned off are determined taking into account two intervals, $\left[t_{0(off)} - t_{2(off)}\right]$, and $\left[t_{2(off)} - t_{3(off)}\right]$ (Fig. 8), where

$$t_{2(off)} = t_{0(off)} + t_{d(off)} - \frac{1}{8}\cdot t_{rr}, \quad (34)$$

$$t_{3(off)} = t_{2(off)} + \frac{9}{8}\cdot t_r + t_{Itail}. \quad (35)$$

On the interval $\left[t_{0(off)} - t_{2(off)}\right]$, the current I_C remains equal to I_{C0}, while U_{ce} increasing, starting from its saturation value in accordance with the expression

$$U_{ce}(t) = U'_{1(off)}\cdot t + U_{ces}\cdot e^{-\lambda_{1(off)}\cdot\left(t-t_{1(off)}\right)}, \quad (36)$$

where

$$t_{1(off)} = t_{0(off)} + k_{Ud}\cdot\left(t_{d(off)} - \frac{1}{8}\cdot t_f\right), \quad (37)$$

$$U'_{1(off)} = \frac{0.1\cdot U_{ce0} - U_{ces}}{k_{Ud}\cdot\left(t_{d(off)} - \frac{1}{8}\cdot t_f\right)}, \quad (38)$$

$$\lambda_{1(off)} = \frac{\ln\left|\frac{U_{ce0} - U'_{1(off)}\cdot t_f}{U_{ces}}\right|}{\left(1-k_{Ud}\right)\cdot\left(t_{d(off)} - \frac{1}{8}\cdot t_f\right)}, \quad (39)$$

$$k_{Ud} = \frac{t_{U_d(off)}}{t_{d(off)}}. \quad (40)$$

On the interval $\left[t_{2(off)} - t_{3(off)}\right]$, the current I_C drops in accordance with the expression

$$I_c(t) = I_{1(off)}\cdot \mathrm{e}^{-\alpha_{1(off)}\cdot\left(t-t_{2(off)}\right)^2} + I_{2(off)}\cdot \mathrm{e}^{-\alpha_{2(off)}\cdot\left(t-t_{2(off)}\right)^2}. \quad (40)$$

The value of the slowly fading current component $I_{2(off)}$ is equal to the final current value I_{tail}, shown in fig. 8. Assumed I_{tail} to be proportional to I_{C0}, this is expressed as

$$I_{tail} = k_{1\infty}\cdot I_{c0}, \quad (41)$$

where $k_{I\infty} = [0-1]$ is a factor depending on the design (relative gain) and type (penetrable or non-penetrable) of the IGBT. The value of the component $I_{1(off)}$ is

$$I_{1(off)} = \left(1-k_{1\infty}\right)\cdot I_{c0}, \quad (42)$$

The coefficients $\alpha_{1(off)}$ and $\alpha_{2(off)}$ were found taking into account a certain point of the current curve as

$$\alpha_{1(off)} = \frac{64}{t_f^2}\cdot\ln\left|\frac{1-k_{1\infty}}{0.9-k_{1\infty}}\right|, \quad (43)$$

$$\alpha_{2(off)} = \frac{1}{\left(t_f + t_{tail}\right)^2}\cdot\ln\left|100\cdot k_{1\infty}\right|. \quad (44)$$

The change U_{ce} over this period is obtained by taking into account the voltage drop across the parasitic inductance as a result of the initial rapid drop I_C

$$U_{ce}(t) = U_{ce0} - L_p\cdot\frac{dI_c}{dt} = U_{ce0} + \\ +U_{2(off)}\cdot e^{-\alpha_1(off)\cdot\left(t-t_{2(off)}\right)^2} + U_{3(off)}\cdot e^{-\alpha_2(off)\cdot\left(t-t_{2(off)}\right)^2}, \quad (45)$$

where

$$U_{2(off)} = 2\cdot\alpha_{1(off)}\cdot I_{1(off)}\cdot L_p, \quad (46)$$

$$U_{3(off)} = 2\cdot\alpha_{2(off)}\cdot I_{2(off)}\cdot L_p. \quad (47)$$

Based on the above relations, the curves of the current and voltage of the transistor at the moment of its shutdown were plotted (Fig. 9).

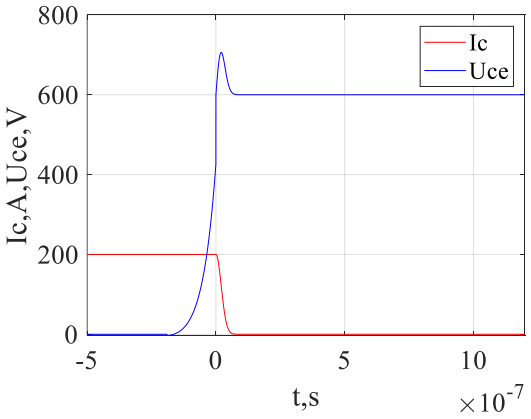

Fig. 6. Curves of current $\left(I_C(t)\right)$ and voltage $\left(U_{ce}(t)\right)$ of the transition process of turning off the transistor.

The energy loss when the transistor is turned off is calculated by the formula

$$W_{off} = \int_{t_{0(off)}}^{t_{3(off)}} U_{ce}(t)\cdot I_c(t)\,dt, \quad (48)$$

By changing the values of the current flowing through the transistor from 50 A to 400 A, at $U_{ce0} = 600\text{V}$, the energy loss curve was plotted when the transistor was turned on (Fig. 10).

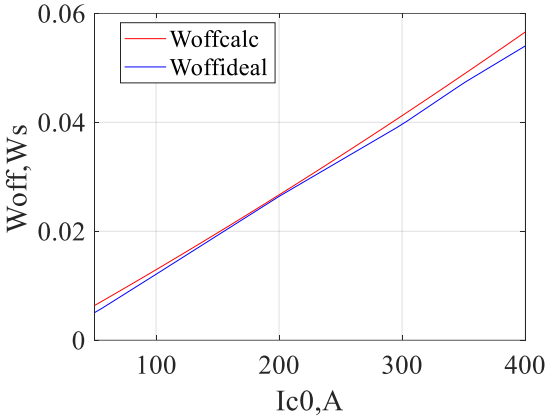

Fig. 10. Energy losses when the transistor is turned on: calculated $(W_{offcalc})$ and passport $(W_{offideal})$.

In fig. 10 is also a curve of energy losses when the transistor is turned off, corresponding to the passport characteristics.

After replacing in formula (16) $W_{reccalc}$ with $W_{offcalc}$ and $W_{recideal}$ with $W_{offideal}$ the error in determining the energy loss when the transistor is turned off, the value of which was $\sigma = 1.5\%$. This indicates a high degree of reliability of the calculated parameters.

From a thermal point of view, IGBT can be represented as a lumped-parameter equivalent circuit (Fig. 11). P_{Lj} are the power losses in the device, moreover, T_j and T_c are the junction and case temperatures, respectively. Nodal voltages correspond to intermediate temperatures inside the device. R_{thi} and C_{thi} represent the thermal resistance and capacitance of the different layers of the semiconductor device. The number of RC chains is usually determined by the number of significantly different layers in the heat path. It is often sufficient to model the radiator as a single lumped heat capacity and resistance from the absorber to ambient temperature (T_a). If many devices are installed on a common radiator, the IGBT thermal equivalent circuit can be connected together with the radiator thermal equivalent, as shown in Fig. eleven.

In fig. 11, T_{ci} is the temperature of the case i of the device mounted on the radiator, and R_{cis} is the corresponding thermal resistances between the case and the radiator. To obtain the transition temperatures, the equations of the state space of the above equivalent thermal scheme are obtained and solved. In order to calculate the average power loss P_{Lj} over a small measurement period, the total energy $(W_{cond} + W_{on} + W_{off} + W_{blok})$ described above is continuously calculated and divided by this measurement period. This measurement period is actually a time step for modeling the equivalent thermal circuit in Fig. eleven.

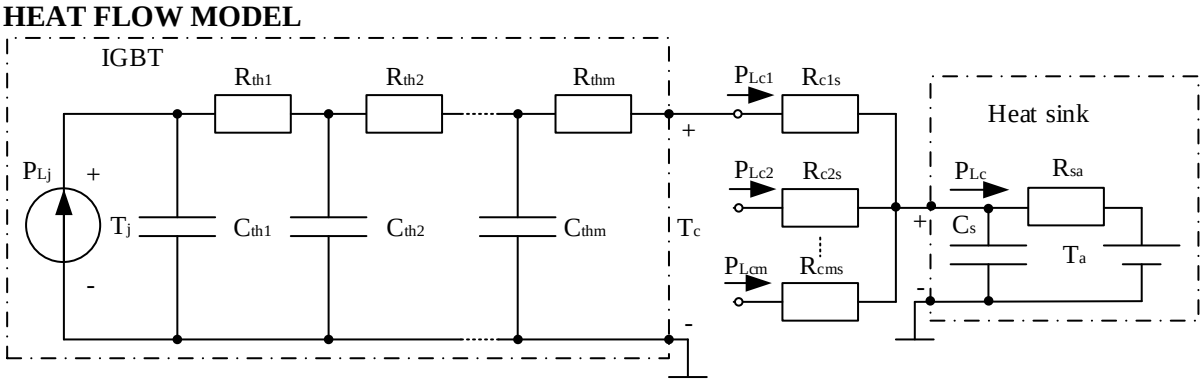

Fig. 11. Equivalent thermal circuit of a semiconductor device and a radiator.

Although some manufacturers list values for R_{thi} and C_{thi} in their device specifications, the information needed to obtain thermal circuit parameters is usually provided in the form of the transient thermal resistance curve (Z_{th}) shown in Fig. 12.

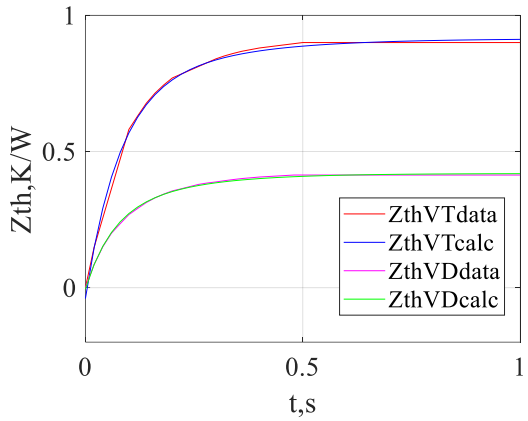

Fig. 12. Transient thermal resistance curves: passport $(Z_{thVTdata})$ and calculated $(Z_{thVTcalc})$ value for the transistor; passport $(Z_{thVDdata})$ and calculated $(Z_{thVDcalc})$ value for the diode.

This curve is approximated by an analytic function [18], which has the form

$$Z_{th}(t) = a_0 + \sum_{i=1}^{n} a_i \cdot e^{-b_i \cdot t}, \quad (49)$$

where $a_0,...,a_n$ and $b_0,...,b_n$ are constants, which are determined using the appropriate curve fitting technique [18]. As a rule, two exponential terms (i.e. $n = 2$, in (49)) can approximate the Z-curve quite accurately.

The results of the approximation of the curves of the transient thermal resistance of the transistor $(Z_{thVTcalc})$ and diode $(Z_{thVDcalc})$ are shown in Fig. 12. The approximation error of the transient thermal resistance curve of the transistor was $\sigma_{VT} = 0.38\%$, diode $\sigma_{VD} = 0.15\%$, which indicates a high reliability of the results obtained.

Then the values R_{thi} and C_{thi} are obtained from a_i and b_i:

$$R_{th1} = \frac{q^2}{q \cdot r - p \cdot s}, \quad (50)$$

$$R_{th2} = p - \frac{q^2}{q \cdot r - p \cdot s}, \quad (51)$$

$$C_{th1} = \frac{s}{q}, \quad (52)$$

$$C_{th2} = \frac{(q \cdot r - p \cdot s)^2}{q \cdot (p \cdot q \cdot r - s \cdot p^2 - q^2)}, \quad (53)$$

where

$$p = a_0, \quad (54)$$

$$q = a_0 \cdot \left(\frac{1}{b_1} + \frac{1}{b_2}\right) + a_1 \cdot \frac{1}{b_1} + a_2 \cdot \frac{1}{b_2}, \quad (55)$$

$$r = \frac{1}{b_1} + \frac{1}{b_2}, \quad (56)$$

$$s = \frac{1}{b_1 \cdot b_2}. \quad (57)$$

The calculation results are summarized in Table 3.

Table 3.

IGBT Heat Flow Model Parameters

Parameter	Device	
	Diode	Transistor
a_0	0.4191	0.9146
a_1	-0.2387	-0.7087
a_2	-0.1804	-0.2059
b_1	17.1237	13.2473
b_2	5.7732	4.4238
R_{th1}	0.3437	0.8020
R_{th2}	0.0754	0.1126
C_{th1}	0.1981	0.1023
C_{th2}	1.9693	1.8454

There are 2 IGBT modules (single-phase modules) in the autonomous voltage inverter on the DC-3 electric locomotive. In total, the inverter uses 3 radiators $570 \times 450 \times 15\text{mm}$. Radiator dimensions, i.e. radiator surface area $S = 0.2565\text{m}^2$, thickness $d = 0.15\text{m}$. The radiator is made from aluminium. Aluminum thermal conductivity coefficient $\lambda = 2.37\text{W}/(\text{m} \cdot {}^\circ\text{C})$, heat capacity coefficient $C_p = 483.6\text{J}/(\text{kg} \cdot {}^\circ\text{C})$, aluminum density $\rho = 2698.72\text{kg}/\text{m}^3$. The thermal resistance of the radiator and the thermal capacity are calculated using the formulas

$$R_{sa} = \frac{d}{\lambda \cdot S}, \quad (58)$$

$$C_{sa} = \frac{1}{C_p \cdot m} = \frac{1}{C_p \cdot \rho \cdot S \cdot d}. \quad (59)$$

Before installing the IGBT module on the radiator, the plane of the module $(S_1 = 0.0065\text{m}^2)$, which is installed on the radiator, is treated with KPT-8 thermal paste. Layer thickness is $d_1 = 0.5\text{mm}$. Thermal conductivity coefficient of aluminum is

$\lambda_1 = 0.65\text{W}/\left(\text{m}\cdot{}^\circ\text{C}\right)$. The thermal resistance of the thermal paste was calculated using the formula

$$R_{c1s} = \frac{d_1}{\lambda_1 \cdot S_1}. \qquad (60)$$

Water with antifreeze is used as a cooling medium in a stand-alone voltage inverter. Coolant sluices are located around the perimeter of the radiator. Under normal operating conditions, the temperature at the entrance to the locks is 25 °C, at the exit – 55 °C. Since the IGBT modules are located in the center of the radiator symmetrically from its geometric center, the average temperature value is taken as the temperature of the cooling medium, i.e. $T_a = 40^\circ\text{C}$.

THERMAL INVERTER MODEL AND SIMULATION RESULTS

When compiling the simulation model, the factor was taken into account that the load of the autonomous voltage inverter is two traction induction motors. In an autonomous voltage inverter, pulse-width modulation with a maximum frequency is used. Therefore, when calculating the losses, the time reciprocal to this frequency was chosen as the time of the measurement period, i.e. $1 = 1/f_{max} = 2\text{ms}$.

Simulation modeling was performed in the MATLab software environment (Fig. 13), using the inverter and traction motor models given in other studies. The electrical part of the model of the traction induction motor of the DC-3 electric locomotive is made using the electrical elements of the Simsape library (Goolak S., Liubarskyi B., Sapronova S., Tkachenko V., Riabov I., Glebova M. Improving a model of the induction traction motor operation non-symmetric stator windings, *Eastern-European Journal of Enterprise Technologies*, 2021, vol. 4, no 8 (112), pp. 45-58. doi:10.15587/1729-4061.2021.236825).

All other parts of the motor are made using the structural elements of the Simulink library. In fig. 13 traction motors are designated as "Induction traction motor 1" and "Induction traction motor 2". The three-phase autonomous voltage inverter is made according to the bridge circuit on IGBT modules. Its model is given in [19, 20]. Block for determining losses, which implements the corresponding expressions given above, is executed on the structural elements of the Simulink library. The block that implements the circuit (Fig. 11) is made using the electrical elements of the Simsape library. These two blocks are combined into one (in Fig. 13 "IGBT module temperature detection unit").

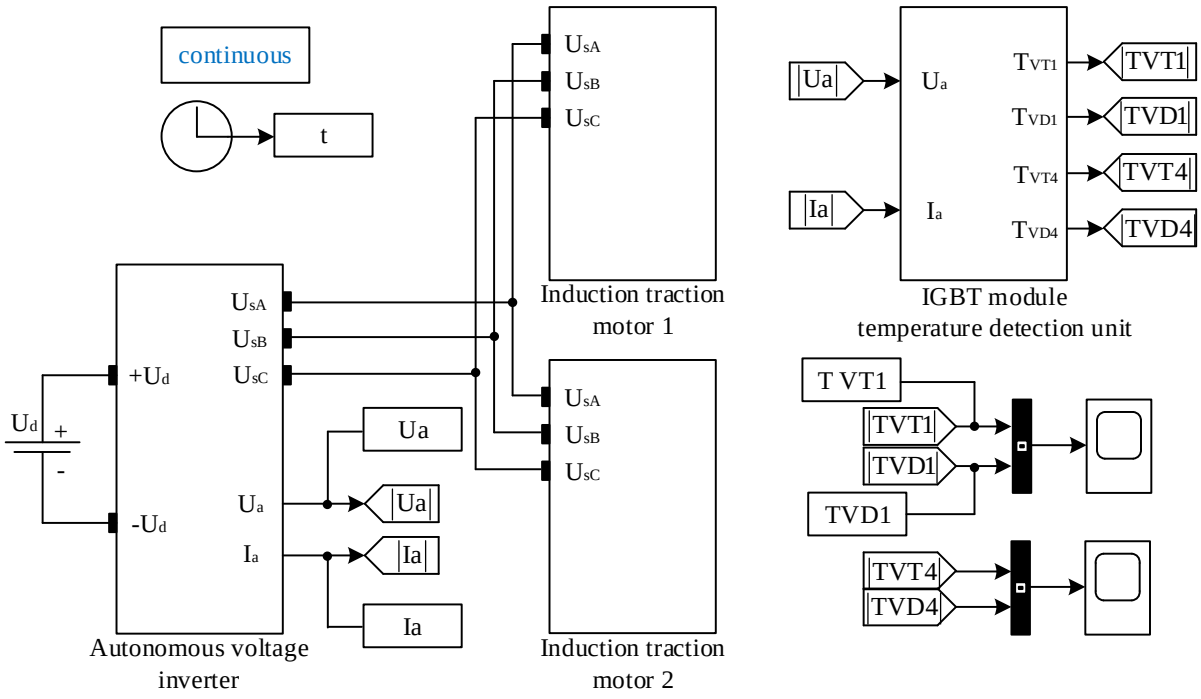

Fig. 13. Simulation model for temperature detection in IGBT voltage inverter modules.

Modeling of thermal processes in an autonomous voltage inverter showed that with symmetrical modes of motor windings and with symmetry of the phases of the inverter, the temperature of the elements of the IGBT modules of all phases is the same. Therefore, Fig. 13 shows 2 IGBT modules that implement phase A of the inverter. Since the temperatures of both diodes and both transistors are equal, in Fig. 14 shows the temperature values of the diode and the transistor of one arm of the inverter for the steady state operation of the motors.

As seen from fig. 14, the temperature value of the transistor VT1 was $T_{VT1} = 113^{\circ}\mathrm{C}$, for the diode VD1 – $T_{VD1} = 69^{\circ}\mathrm{C}$. According to the passport data of the DC-3 electric locomotive, the operating range of the IGBT transistor of the autonomous voltage inverter module operating in nominal mode is from 110 °C to 125 °C, the diode is from 65 °C to 125 °C.

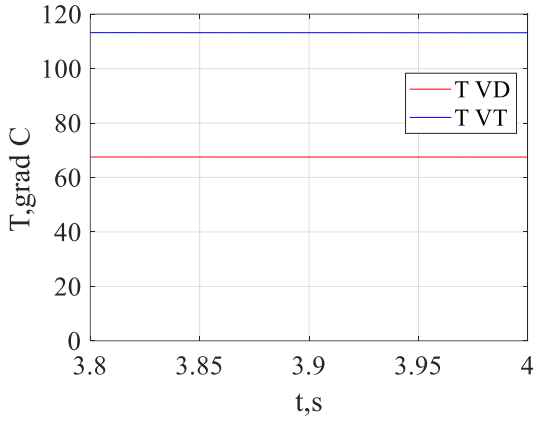

Fig. 14. The temperature value of the transistor VT1 (T_{VT}) and the diode VD1 (T_{VD}) in the steady state of the motors.

Since the corresponding simulation results fell within the indicated ranges, it can be said that the simulation results obtained using the developed thermal model of an autonomous voltage inverter are highly reliable.

CONCLUSIONS

The paper proposes a thermal model of the output converter of an electric locomotive with vector control of induction traction motors. To solve this problem, the following was done:

- The structure of the thermal model of the output converter has been developed;
- Modeling of heat losses in the IGBT module in the stationary mode and switching mode has been performed. For this purpose, the switching periods of electronic devices are divided into characteristic time intervals. For these intervals, integrable functions are proposed that describe the curves of currents and voltages in these sections. The energy losses are calculated when the transistor is turned on, when the transistor and diode are turned off. Comparison of the results of energy calculations with passport characteristics showed a high reliability of the results obtained. Thus, the error in determining the energy loss when the transistor is turned on did not exceed 1.5%, when the transistor was turned off, it did not exceed 3.77%, and when the diode was turned off, it did not exceed 0.12. For a period of time corresponding to the reciprocal of the maximum PWM sampling frequency, the power losses are calculated;
- Using the calculated power losses in the IGBT module, a circuit for determining the temperature of the electronic devices of the module has been developed. To obtain the values of the circuit elements, the passport characteristics of the thermal resistance curve of the transistor and diode were approximated by exponential functions. The values of the circuit elements are calculated using the obtained coefficients of the approximating function;
- Simulation modeling of temperature determination in IGBT inverter modules was performed, the load of which was two traction motors of the DC-3 electric locomotive operating in the nominal mode. For the steady state operation of the motors, the temperatures of the transistor and diode of one arm of phase A were obtained. As a result of the simulation, it was found that under the conditions of symmetry of the stator windings of all motors and the symmetry of the output voltages of the inverter, the temperatures of all transistors will be equal. The temperatures of all diodes will also be equal. The temperature values were: transistor 113 °C, diode 69 °C. Comparison of the obtained results with the passport characteristics of the DC-3 electric locomotive indicates the adequacy of the results obtained.

References

[1] Hassan M. M., Shaikh M. S., Jadoon H. U. K., Atif M. R., Sardar, M. U. Dynamic Modeling and Vector Control of AC Induction Traction Motor in China Railway. *Sukkur IBA Journal of Emerging*

Technologies, 2020, vol. 3, no 2, pp. 115-125. Available at: doi: 10.30537/sjet.v3i2.622

[2] Farah N., Talib M. H., Ibrahim Z., Abdullah Q., Aydoğdu Ö., Rasin Z., *Jidin A.* & Lazi, J. M. Analysis and investigation of different advanced control strategies for high-performance induction motor drives. *TELKOMNIKA (Telecommunication Computing Electronics and Control)*, 2020, vol. *18*, *no* 6, pp. 3303-3314. Available at: doi: 10.12928/telkomnika.v18i6.15342

[3] Maghfiroh H., Pramono S., Hermanu C., Nizam M. Comparative Study of PWM Method for Optimal Energy Control of Railway Traction Motor. In *2018 5th International Conference on Electric Vehicular Technology (ICEVT), 2018*, pp. 199-203. IEEE. Available at: doi: 10.1109/ICEVT.2018.8628419

[4] Poorfakhraei A., Narimani M., Emadi A.. A review of modulation and control techniques for multilevel inverters in traction applications. *IEEE Access*, 2021, vol. *9*, pp. 24187-24204. Available at: doi: 10.1109/ACCESS.2021.3056612

[5] Menon R., Azeez N. A., Kadam A. H., Williamson S. S. Energy loss analysis of traction inverter drive for different PWM techniques and drive cycles. In *2018 IEEE International Conference on Industrial Electronics for Sustainable Energy Systems (IESES)*, 2018, pp. 201-205. IEEE. Available at: doi: 10.1109/IESES.2018.8349874

[6] Aryza S., Irwanto M., Lubis Z., Siahaan A. P. U., Rahim R., Furqan M. A Novelty Design Of Minimization Of Electrical Losses In A Vector Controlled Induction Machine Drive. In *IOP Conference Series: Materials Science and Motorering*, 2018, vol. 300, no. 1, p. 012067. IOP Publishing. Available at: doi: 10.1088/1757-899X/300/1/012067.

[7] Popov A. N. Energy-saving Regulators for Asynchronous Electric Drive Vector Control Systems: Design Procedure and Adaptive Control. In *2019 26th International Workshop on Electric Drives: Improvement in Efficiency of Electric Drives (IWED)*, 2019, pp. 1-4. IEEE. Available at: doi: 10.1109/IWED.2019.86642559.

[8] Ismail A., Saidi L., Sayadi M., Benbouzid M. Gaussian process regression remaining useful lifetime prediction of thermally aged power IGBT. In *ECON 2019-45th Annual Conference of the IEEE Industrial Electronics Society*, 2019, vol. 1, pp. 6004-6009. IEEE. Available at: doi: 10.1109/IECON.2019.8926710.

[9] Goolak S., Tkachenko V., Sapronova S., Lukoševičius V., Keršys R., Makaras R., Keršys A., Liubarskyi B. Synthesis of the Current Controller of the Vector Control System for Asynchronous Traction Drive of Electric Locomotives. *Energies*, 2022, vol. 15, no 7, pp. 2374-2392. Available at: doi: 10.3390/en15072374

[10] Zhang C., Yu S., Ge X. A stationary-frame current vector control strategy for single-phase PWM rectifier. *IEEE Transactions on Vehicular Technology*, 2019, vol. 68, no 3, pp. 2640-2651. Available at: doi: 10.1109/WiPDAAsia.2018.8734624

[11] Górecki K., Zarębski J., Górecki P., Ptak P. Compact thermal models of semiconductor devices–a review. *International Journal of Electronics and Telecommunications*. 2019. vol. 65, no 2, pp. 151-158. Available at: doi: 10.24425/ijet.2019.126295

[12] Wang B. Research on Electro-thermal Model Simulation of IGBT Switching Transient. In *IOP Conference Series: Earth and Environmental Science* , 2021, vol. 702, no. 1, p. 012037. IOP Publishing. Available at: doi: 10.1088/1755-1315/702/1/012037

[13] Wang J., Chen W., Wang L., Wang B., Zhao C., Ma D., Yang. F.. Li, Y.. A Transient 3-D Thermal Modeling Method for IGBT Modules Considering Uneven Power Losses and Cooling Conditions. *IEEE Journal of Emerging and Selected Topics in Power Electronics*, 2020, vol. 9, no 4, pp. 3959-3970. Available at: doi: 10.1109/JESTPE.2020.3021679

[14] Górecki P., Górecki K., Zarębski J. Thermal model of the IGBT module. In *Journal of Physics: Conference Series*, 2018, vol. 1033, no. 1, p. 012001. IOP Publishing. Available at: doi: 10.1088/1742-6596/1033/1/012001

[15] Zhang Y., Wang H., Wang Z., Yang Y., Blaabjerg F. Simplified thermal modeling for IGBT modules with periodic power loss profiles in modular multilevel converters. *IEEE Transactions on Industrial Electronics*, 2018, vol. 66, no. 3, pp. 2323-2332. Available at: doi: 10.1088/1742-6596/1033/1/012001

[16] Chen X., Huang S., Li, B., Xiang Y. Losses and thermal calculation scheme of IGBT and FWD and its application in PWM inverters for electric motorering maintenance rolling stock. *IEEJ Transactions on Electrical and Electronic Motorering*, 2018, vol. *13, no.* 12, pp. 1822-1828. Available at: doi: 10.1109/TIE.2018.2823664

[17] Sun B., Zhang Z., Andersen M. A. A comparison review of the resonant gate driver in the silicon MOSFET and the GaN transistor application. *IEEE Transactions on Industry Applications*, 2019, vol. *55*, no. 6, pp. 7776-7786. Available at: doi: 10.1109/TIA.2019.2914193

[18] Chen H., Chillotti I., Song, Y. Improved bootstrapping for approximate homomorphic encryption. In *Annual International Conference on the Theory and Applications of Cryptographic Techniques*, 2019, pp. 34-54. Springer, Cham. Available at: doi: 10.1007/978-3-030-17656-3_2

[19] Plakhtii O., Nerubatskyi V., Mykhalkiv S., Hordiienko D., Shelest D., Khomenko I.. Research of Energy Characteristics of Three-Phase Voltage

Source Inverters with Modified Pulse Width Modulation. In *2021 IEEE 2nd KhPI Week on Advanced Technology (KhPIWeek)*, 2021, pp. 422-427. IEEE. Available at: doi: 10.1109/KhPIWeek53812.2021.9570071

[20] Plakhtii O., Tsybulnyk V., Nerubatskyi, V., Mittsel N. The analysis of modulation algorithms and electromagnetic processes in a five-level voltage source inverter with clamping diodes. In *2019 IEEE International Conference on Modern Electrical and Energy Systems (MEES)*, 2019, pp. 294-297. IEEE. Available at: doi: 10.1109/MEES.2019.8896567

Сведения об авторах.

Гулак Сергей Александрович, к.т.н., Киевский институт железнодорожного транспорта Государственного университета инфраструктуры и технологий. Область научных интересов – математическое моделирование систем управления тяговыми приводами электровозов.
E-mail: sgoolak@gmail.com

Кириченко Михаил Анатольевич, к.т.н., Национальный университет строительства и архитектуры. Область научных интересов – математическое моделирование термодинамических процессов.
E-mail: kirichenkom@ukr.net